

## MATHEMATICAL MODELING OF THE INTRUSION OF SEA WATER INTO LITTORAL SWEET-WATER HORIZONS

É. N. Bereslavskii

UDC 532.546

*Consideration has been given to mathematical models of certain two-dimensional, steady-state filtration flows of sweet groundwater from a reservoir (water storage), via a rectangular pressure water-bearing stratum, to a sea with saline water overlain by a sweet water layer. The algorithm of calculation of the intrusion of sea saline water into littoral sweet-water strata where groundwater flows enter the sea from the side (scheme of Polubarinova-Kochina and Mikhailov) or from below (Bear–Dagan scheme) have been developed based on these models.*

**Introduction.** Interpretation of the boundary between a filtered liquid and a basin with a heavier liquid as an analog of a seepage gap was proposed for the first time in [1]. This work was the starting point toward further investigations of problems of such kind. Mathematical models of filtration of sweet groundwater in a semiinfinite horizontal pressure layer to a sea with saline water overlain by sweet water were considered in [2, 3]. Below, we study the cases of motion via a rectangularly shaped homogeneous stratum of finite dimensions; we consider two forms of flow: when groundwater enters the sea from the side (Polubarinova-Kochina and Mikhailov scheme) and from below (Bear–Dagan scheme). To solve the problems we use the Polubarinova-Kochina method [4] based on the application of the theory of Fuks linear differential equations [5]. Using the exact analytical dependences obtained and numerical calculations, we analyze the influence of each physical parameter of the models on geometric and filtration characteristics and study the distinctive features of filtration, which finally gives a comprehensive picture of the phenomena. Limiting cases of flows are considered. It has been shown that, for certain particular values of the unknown parameters of a conformal mapping, which are contained in the solution, the latter yields the well-known results of P. Ya. Polubarinova-Kochina for the classical problem on filtration in a rectangular bridge [4, 6–8]. In the particular case where the layer of sweet water above the sea table is absent, we compare results of calculations for both schemes of inflow.

**Scheme of Lateral Inflow. Formulation of the Problem and Its Solution.** Sweet water of density  $\rho_1$  moving from a reservoir in a rectangular pressure water-bearing stratum of thickness  $T$  and width  $L$  (located on an impermeable rock-salt layer) enters a sea with a denser saline water of density  $\rho_2$  ( $\rho_2 > \rho_1$ ). Above the saline-water horizon, there is a layer of less dense sweet water in the sea with a level  $t$  ( $0 < t \leq T$ ). The initially vertical boundary line between the moving sweet water and the a quiescent saline water begins to change its shape in the lower right-hand part of the stratum under pressure (head)  $H$ , shifting to the left toward the flow. After a certain period, we may have a steady-state motion [6, 9], when the brine settles down, the boundary turns out to be a streamline for the sweet water, and the motion of the sea water toward the land takes on the shape of a salt-water wedge (or tongue) penetrating into the sweet-water stratum (Fig. 1). This phenomenon is called the intrusion (penetration) of saline water [10].

We will assume that the motion of groundwater obeys Darcy's law with a known coefficient of filtration  $\kappa = \text{const}$  and occurs in a homogeneous isotropic ground which is considered as being incompressible, just as the liquid filtered through it. The influence of capillary and diffusion phenomena at the boundary is disregarded, as is the case in problems of such kind [1, 4, 6, 9–11].

Under such assumptions traditional for the class of flows in question, mathematical modeling of the filtration process under study is reduced to finding the complex flow potential  $\omega(z)$  with the following boundary conditions:

---

Academy of Civil Aviation, 38 Piloty Str., St. Petersburg, 196210, Russia, email: beres@nwgsm.ru. Translated from *Inzhenerno-Fizicheskii Zhurnal*, Vol. 79, No. 5, pp. 126–134, September–October, 2006. Original article submitted February 1, 2005.

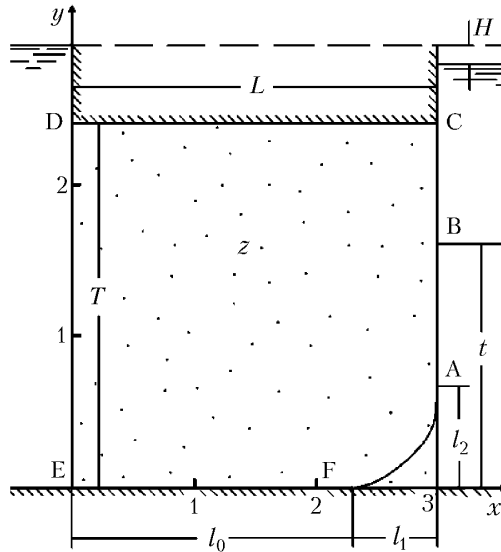


Fig. 1. Form of lateral inflow, calculated for  $T = 2.4$  m,  $L = 3.0$  m,  $\rho = 0.01$ ,  $H = 0.036$  m, and  $t = 1.5861$  m.  $x, y$ , m

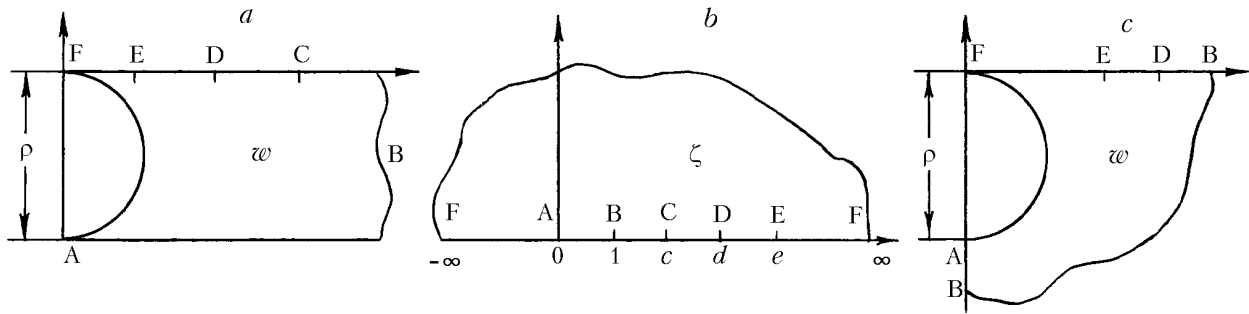


Fig. 2. Regions of complex velocity for the scheme of lateral inflow (a), auxiliary parametric variable (b), and complex velocity for the scheme of inflow from below (c)

$$AB: x=L, \quad \varphi = \rho(y-t); \quad BC: x=L, \quad \varphi = 0;$$

$$CD: y=T, \quad \varphi = Q; \quad DE: x=0, \quad \varphi = -H;$$

$$EF: y=0, \quad \varphi = 0; \quad FA: \varphi = \rho(y-t), \quad \phi = 0, \quad \rho = \frac{\rho_2}{\rho_1} - 1. \quad (1)$$

Here  $\varphi$  and  $\phi$  are the mutually conjugate functions harmonic within the region  $z = x + iy$ : the velocity potential and the stream function referred to  $\kappa$ ;  $Q$  is the total filtration flow rate referred to  $\kappa$  also. It is desired to determine the position of the boundary line AF and consequently the width  $l_1$  and the height  $l_2$  of the saline-water wedge penetrated into the stratum.

We now direct our attention to the region of the complex velocity  $w$  corresponding to boundary conditions (1). This region is shown in Fig. 2a and has the same form as that in [2, 3]; therefore, the conformal mapping of the upper half-plane of the auxiliary parametric variable  $\zeta$  (the correspondence of points is shown in Fig. 2b) onto the region  $\omega$  retains its form

$$w = \rho \frac{K(\zeta) - iK'(\zeta)}{K'(\zeta)}, \quad (2)$$

where  $K(\zeta)$  is the complete elliptic integral of the first kind [4] considered as a function of the modulus squared  $k^2 = \zeta$  and  $K'(\zeta) = K(1 - \zeta) = K(k'^2)$ ,  $k'^2 = 1 - k^2 = 1 - \zeta$ . However, three unknown affixes corresponding respectively to the angular points C, D, and E of the region of flow are now contained (compared to [2, 3]) on the region contour. The total number of singular points reaches six, so that it becomes much more difficult to solve the problem computationally. We recall that the number of singular points in the problem of filtration in a rectangular bridge [4, 6, 7] was equal to five.

We use the Polubarinova-Kochina method [4] to solve the problem. We introduce the function  $z(\zeta)$  conformally mapping the upper half-plane  $\zeta$  onto the region  $z$ , the complex velocity  $w = d\omega/dz$ , and the derivatives

$$Z = \frac{dz}{d\zeta}, \quad \Omega = \frac{d\omega}{d\zeta}. \quad (3)$$

Using the procedure for determining the exponents of the functions  $Z$  and  $F$  near singular points [4, 12] and allowing for expression (2), we find

$$Z = \frac{AiK'(\zeta)}{\Delta(\zeta)}, \quad \Omega = A\rho \frac{K'(\zeta) + iK(\zeta)}{\Delta(\zeta)}, \quad \Delta(\zeta) = \sqrt{(\zeta - c)(\zeta - d)(\zeta - e)}, \quad (4)$$

where  $A$  is the unknown scale constant. It is noteworthy that the function  $K'(\zeta)$  is the solution containing a logarithmic singularity at the point  $\zeta = 0$  in whose vicinity an asymptotic representation has the form [13]  $K'(\zeta) = -0.5 \ln \zeta$ . We may assure that the functions (4) satisfy boundary conditions (1) formulated in terms of the functions mentioned and hence are the parametric solution of the initial boundary-value problem.

Writing the representations (4) for different portions of the boundary of the region  $\zeta$  followed by integration over the entire contour of the auxiliary region yields the parametric equations of the corresponding portions of the flow diagram. As a result, we obtain an expression for the determining physical parameters of the model  $L$ ,  $H$ ,  $T$ , and  $t$  and the coordinates of the points of the boundary line AF.

The main computational difficulty of the problem is that the integrands appearing in the relations sought have (as has already been mentioned) logarithmic singularities in the vicinity of the point  $\zeta = 0$ ; furthermore, they are infinite on the limits of integration.

For convenience of computations, we introduce the notation  $\alpha = \frac{1}{d}$ ,  $\beta = \frac{1}{c}$ , and  $\gamma = \frac{1}{e}$  ( $0 \leq \gamma \leq \alpha < \beta \leq 1$ ) and, following [4, p. 278], replace  $\zeta$  by the corresponding expressions for different intervals, owing to which the integrands are finite on the limits of integration:

$$\zeta = \tau (0 < \zeta < 1), \quad \tau = \sin^2 t, \quad \zeta = 1 - \frac{1}{\tau} (-\infty < \zeta < 0), \quad \tau = \cos^2 t,$$

$$\zeta = \frac{1}{\tau} (1 < \zeta < c), \quad \tau = \beta + (1 - \beta) \sin^2 t, \quad (c < \zeta < d) \tau = \alpha + (\beta - \alpha) \sin^2 t,$$

$$(d < \zeta < e) \tau = \gamma + (\alpha - \gamma) \sin^2 t, \quad (e < \zeta < \infty) \tau = \gamma \sin^2 t.$$

As a result, we arrive at the following calculated dependences ( $C = 2A\sqrt{\alpha\beta\gamma}$ ,  $\alpha_1 = 1 - \alpha$ ,  $\beta_1 = 1 - \beta$ , and  $\gamma_1 = 1 - \gamma$ ):

$$L = C \int_0^{\pi/2} \frac{K[\alpha_1 - (\beta - \alpha) \sin^2 t] dt}{\sqrt{\alpha - \gamma + (\beta - \alpha) \sin^2 t}}, \quad H = C\rho \int_0^{\pi/2} \frac{K[\alpha + (\beta - \alpha) \sin^2 t] dt}{\sqrt{\alpha - \gamma + (\beta - \alpha) \sin^2 t}}; \quad (5)$$

$$T = C \int_0^{\pi/2} \frac{K[\gamma_1 - (\alpha - \gamma) \sin^2 t] dt}{\sqrt{\beta - \gamma - (\alpha - \gamma) \sin^2 t}}, \quad t = T - C\sqrt{\beta_1} \int_0^{\pi/2} \frac{K(\beta_1 \cos^2 t) \cos t dt}{\sqrt{(\beta - \alpha + \beta_1 \sin^2 t)(\beta - \gamma + \beta_1 \sin^2 t)}}; \quad (6)$$

$$x(t) = l_0 + C \int_0^t \frac{K(\sin^2 t) \sin t \cos t dt}{\sqrt{(1 - \alpha_1 \sin^2 t)(1 - \beta_1 \sin^2 t)(1 - \gamma_1 \sin^2 t)}},$$

$$l_0 = C \sqrt{\gamma} \int_0^{\pi/2} \frac{K(1 - \gamma \sin^2 t) \sin t dt}{\sqrt{(\beta - \gamma \sin^2 t)(\alpha - \gamma \sin^2 t)}}, \quad (7)$$

$$y(t) = C \int_0^t \frac{K(\cos^2 t) \sin t \cos t dt}{\sqrt{(1 - \alpha_1 \sin^2 t)(1 - \beta_1 \sin^2 t)(1 - \gamma_1 \sin^2 t)}}, \quad 0 \leq t \leq \frac{\pi}{2};$$

$$l_1 = x\left(\frac{\pi}{2}\right) - l_0, \quad l_2 = y\left(\frac{\pi}{2}\right); \quad (8)$$

$$Q_{BC} = C\rho \sqrt{\beta_1} \int_0^{\pi/2} \frac{K(\beta + \beta_1 \sin^2 t) \cos t dt}{\sqrt{(\beta - \alpha + \beta_1 \sin^2 t)(\beta - \gamma + \beta_1 \sin^2 t)}},$$

$$Q = C\rho \int_0^{\pi/2} \frac{K(\gamma + (\alpha - \gamma) \sin^2 t) dt}{\sqrt{\beta - \gamma - (\alpha - \gamma) \sin^2 t}}. \quad (9)$$

Calculation is controlled by other expressions for the quantities  $l_1$ ,  $l_2$ , and  $Q_{BC}$ ,  $H - \rho t$ :

$$l_1 = L - l_0, \quad l_2 = t - C \int_0^{\pi/2} \frac{K(\cos^2 t) \sin t \cos t dt}{\sqrt{(1 - \alpha \sin^2 t)(1 - \beta \sin^2 t)(1 - \gamma \sin^2 t)}}, \quad (10)$$

$$Q_{BC} = Q - C\rho \int_0^{\pi/2} \frac{K(\sin^2 t) \sin t \cos t dt}{\sqrt{(1 - \alpha \sin^2 t)(1 - \beta \sin^2 t)(1 - \gamma \sin^2 t)}}, \quad (11)$$

$$H - \rho t = C\rho \sqrt{\gamma} \int_0^{\pi/2} \frac{K(\gamma \sin^2 t) \sin t dt}{\sqrt{(\beta - \gamma \sin^2 t)(\alpha - \gamma \sin^2 t)}}. \quad (12)$$

**Calculation of the Flow Diagram and Analysis of Numerical Results.** The dimensions of the wedge  $l_1$  (curves 1) and  $l_2$  (curves 2) as functions of the determining physical characteristics  $T$ ,  $\rho$ ,  $H$ ,  $L$ , and  $t$  are presented by the solid curves in Fig. 3. An analysis of the plots leads us to the following conclusions.

The same qualitative character of the dependences of  $l_1$  and  $l_2$  on the parameters  $T$ ,  $\rho$ ,  $H$ ,  $L$ , and  $t$  is noteworthy: the increase in the dimensions of the stratum and in the density of saline water and the thickness of its layer in the sea leads to a growth in the dimensions of the saline-water wedge. From Fig. 3a it is clear that the dependences of  $l_1$  and  $l_2$  on  $T$  are qualitatively similar with increase in the thickness; the quantities  $l_1$  and  $l_2$  increase nearly to the same extent (3.7 to 3.8 times). Analogous changes (of 3.1 to 3.6 times) are also tracked with variation of the parameters  $H$ ,  $\rho$ , and  $t$ . The relative dimensions of the wedge may be quite considerable: it follows from the calculations that we have  $l_2 = 1.6962$  for  $T = 2.4$ ,  $L = 6.0$ , and  $\rho = 0.01$  and obtain  $l_1 = 1.7274$  for  $T = 2.4$ ,  $L = 3.0$ ,  $\rho = 0.014$ , i.e., the height and width of the wedge may attain 70.7 and 58%, respectively, of the thickness and width of the stratum.

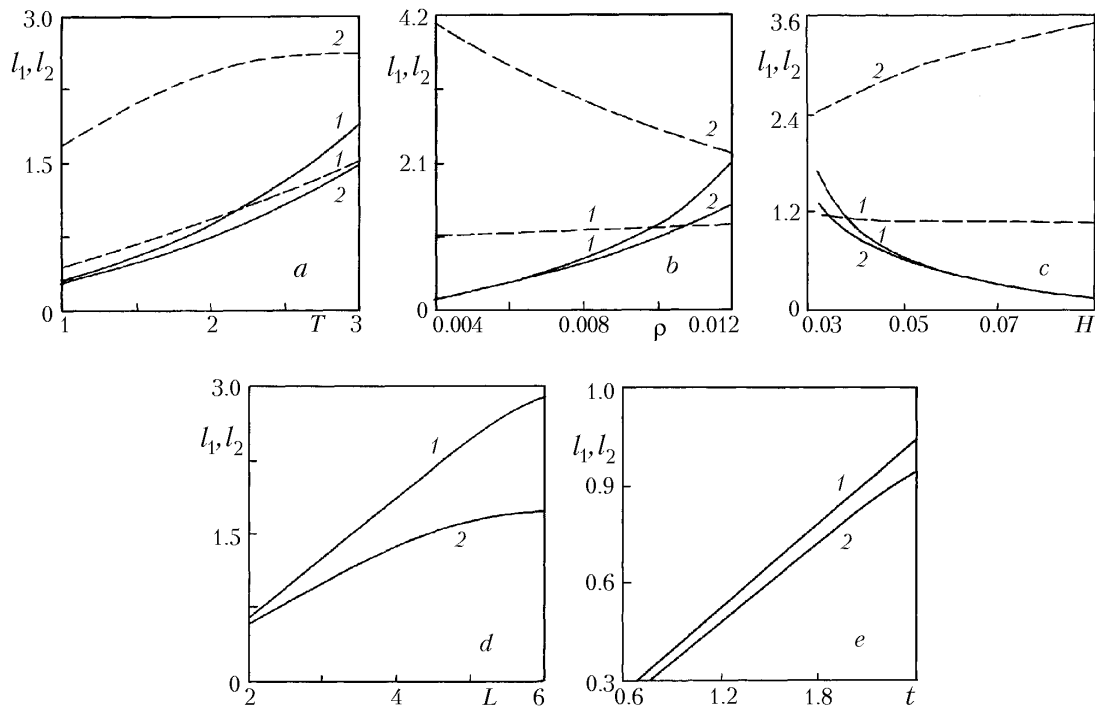


Fig. 3. Dependence of  $l_1$  and  $l_2$  on  $T$  (a),  $\rho$  (b),  $H$  (c),  $L$  (d), and  $t$  (e) for  $L = 3.0$  m,  $\rho = 0.01$ ,  $H = 0.036$  m,  $t = 1.5861$  m, and  $T = 2.4$  m: 1) corresponds to  $l_1$ , 2) to  $l_2$ ; solid curves, scheme of lateral inflow, dashed curves, scheme of inflow from below.  $l_1$ ,  $l_2$ ,  $H$ ,  $L$ ,  $t$ , and  $T$ , m

Just the opposite qualitative character of the dependences of the dimensions  $l_1$  and  $l_2$  on the parameters  $\rho$  and  $H$  is in evidence. Whereas an increase in the density of saline water increases the dimensions of the wedge (Fig. 3b) and decreases the flow rates  $Q_{BC}$  and  $Q$ , such a change is, conversely, brought about by a decrease in the acting head (Fig. 3c). A substantial influence of the dimensions of the wedge  $l_1$  and  $l_2$  is exerted by the width of the stratum. Thus, as the parameter  $L$  increases thrice, the quantities  $l_1$  and  $l_2$  will change by 320.8 and 163.8% respectively (Fig. 3d). It is remarkable for Fig. 3 that the approximate equality  $l_1 \approx l_2$  holds in the case of relatively low values of the parameters  $T$ ,  $\rho$ ,  $L$ , and  $t$  and high values of the parameter  $H$ . And conversely, for high  $T$ ,  $\rho$ ,  $L$ , and  $t$  values and low  $H$  values we have  $l_1 \approx ml_2$ , where  $1.1 \leq m \leq 1.69$ .

Of particular interest is the behavior of the dimensions of the wedge as a function of the thickness of the saline-water layer in the sea. From Fig. 3e it is clear that the dependences of  $l_1$  and  $l_2$  on  $t$  are linear: for the basic variant, we may take  $l_1 = 0.44t - 0.1$  and  $l_2 = 0.4t$ . The width of the wedge is 8 to 12% larger than its height. On the other hand, it is noticeable that, as the level of saline water in the sea increases, the ratio  $l_1/t$  remains virtually constant (43.6%), preserving a certain trend toward decreasing, whereas the ratio  $l_2/t$  decreases from 40.5% for  $t = 0.6893$  to 38.9% for  $t = T$ . The latter means that the larger the thickness of the sweet water above the saline one, the larger the relative dimensions of the saline-water wedge and hence the degree of intrusion.

The calculations show that the rate of flow through segment BC and the total flow rate increase with increase in the parameters  $T$  and  $H$  and decrease in  $L$ ,  $\rho$ , and  $t$ . The  $Q_{BC}/Q$  ratio changes by 51% with increase in the head and, conversely, decreases 1.1 to 1.7 times with increase in all the remaining parameters. It follows from the calculation that, as the depth of saline water in the sea increases,  $Q_{BC}/Q$  decreases from 0.82 for  $t = 0.6893$  to 0 for  $t = T$ .

**Limiting Cases. Solution of P. Ya. Polubarinova-Kochina of the Problem on Filtration in a Rectangular Bridge.** We note particular limiting cases of the filtration scheme in question.

*Flow in the Absence of a Sweet-Water layer above the Sea Surface.* This case corresponds to the points B and C merging together in the  $z$  and  $\zeta$  planes, in which  $t = T$  and  $c = 1$ . The results are obtained from formulas (5)–(12) for  $\beta = 1$  and  $\beta_1 = 0$ ; the second equation of (6) becomes identical, and (9) and (11) yield that  $Q_{BC} = 0$  and  $Q_{AB} = Q$ .

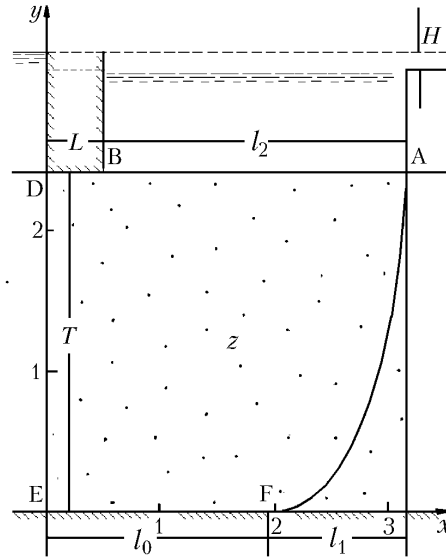


Fig. 4. Form of inflow from below, calculated for  $T = 2.4$  m,  $\rho = 0.01$ ,  $H = 0.036$  m, and  $Q = 0.055$ .  $x, y$ , m

*Flow in a Semiinfinite Layer* [2]. This scheme is obtained from the previous one when points D and E additionally merge together in the  $z$  and  $\zeta$  planes, which corresponds to the values of the parameters  $L = \infty$  and  $d = e$ . The results are obtained from formulas (5)–(12) for  $\beta = 1$ ,  $\beta_1 = 0$ , and  $\alpha = \gamma$ ;  $l_0 = 0$  and  $H = \rho t$  are the permissible values for the physical parameters in the limiting case in question. Expressions (6) and (9) yield that

$$T = C \int_0^{\pi/2} \frac{K(\alpha_1)}{\sqrt{\alpha_1}} dt = \frac{A\pi\alpha K(\alpha_1)}{\sqrt{\alpha_1}} = \frac{A\pi K'(1/d)}{\sqrt{d(d-1)}}, \quad Q = C\rho \int_0^{\pi/2} \frac{K(\alpha)}{\sqrt{\alpha_1}} dt = \frac{A\rho\alpha K(\alpha)}{\sqrt{\alpha_1}} = \frac{A\rho K(1/d)}{\sqrt{d(d-1)}}. \quad (13)$$

Formulas (13) coincide with formulas (2.8) from [2] and are used for determination of unknown parameters from the prescribed values of the physical characteristics  $T$  and  $Q$ .

*Filtration through a Rectangular Bridge. Solution of P. Ya. Polubarinova-Kochina* [4, 6, 7]. When points E and F merge together in the  $z$  and  $\zeta$  planes, i.e., when  $e = \infty$ , which corresponds to a value of  $l_0 = 0$ , the region of flow reduces to the mirror mapping of the region of motion of groundwater in a rectangular bridge. The existing solution of this problem, obtained for the first time by P. Ya. Polubarinova-Kochina ([4], pp. 274–275, formulas (10.34)–(10.43)), follows from formulas (5)–(12) for  $\gamma = 0$ ,  $\alpha = \beta_1$ ,  $\beta = \alpha_1$ , and  $t = \frac{\pi}{2} - \chi$  and after the replacement of the notation  $c, d, L$  (or  $l_1$ ),  $l_2, t - l_2, T, T - t, Q_{AB}$ , and  $Q_{BC}$  by  $a, b, l, H_1 - H_2 - H_0, H_0, H_1, H_2, Q_0$ , and  $Q_2$  respectively.

**Scheme of Inflow from Below. Formulation of the Problem and Its Solution.** Figure 4 shows the traditional [10] diagram of a flow of sweet groundwater in the littoral pressure water-bearing layer; the flow is unloaded into the sea from below. Here the problem is reduced to determination of the complex potential  $\omega(z)$  with boundary conditions (1), with the only difference being that the conditions on portions AB and BC are replaced by the conditions  $y = T$  and  $\varphi = 0$  and  $l_2$  is now the length of the portion where the sweet water passes to the sea floor.

Conformal mapping of the upper half-plane of the auxiliary parametric variable  $\zeta$  (Fig. 2b) onto the complex-velocity region (Fig. 2c) here has the previous expression [2, 3]

$$w = \frac{\pi\rho i}{2 \arcsin \sqrt{1 - \zeta}}. \quad (14)$$

Determining the exponents of the function  $Z$  and  $\Omega$  [4, 12] and allowing for expression (14), we find

$$Z = -\frac{2A}{\pi} \frac{\arcsin \sqrt{1-\zeta}}{\Delta(\zeta)}, \quad \Omega = \frac{A\rho i}{\Delta(\zeta)}, \quad \Delta(\zeta) = \sqrt{\zeta(1-\zeta)(d-\zeta)(e-\zeta)}. \quad (15)$$

Expressions (corresponding to relations (5)–(12)) for the determining parameters of the model take the form

$$L = \frac{2C}{\pi} \int_0^{\pi/2} \frac{\ln [(1 + \sqrt{\alpha_1} \cos t) / \sqrt{\alpha + \alpha_1 \sin^2 t}] dt}{\sqrt{\alpha - \gamma + \alpha_1 \sin^2 t}}, \quad H = \frac{C\rho K}{\sqrt{\gamma_1}}; \quad (16)$$

$$T = \frac{C}{\sqrt{\gamma_1}} F(\arcsin \sqrt{\gamma_1}, k), \quad k = \sqrt{\frac{\alpha_1}{\gamma_1}}, \quad k' = \sqrt{\frac{\alpha - \gamma}{\gamma_1}}; \quad (17)$$

$$x(t) = l_0 + \frac{2C}{\pi} \int_t^{\pi/2} \frac{\ln [(1 + \sin t) / \cos t] \cos t dt}{\sqrt{(1 - \alpha_1 \sin^2 t)(1 - \gamma_1 \sin^2 t)}}, \quad l_0 = \frac{2C \sqrt{\gamma}}{\pi} \int_0^{\pi/2} \frac{\ln [(1 + \sqrt{1 - \gamma \sin^2 t}) / \sqrt{\gamma} \sin t] \sin t dt}{\sqrt{(1 - \gamma \sin^2 t)(\alpha - \gamma_1 \sin^2 t)}},$$

$$y(t) = \frac{C}{\sqrt{\gamma_1}} [F(\arcsin \sqrt{\gamma_1}, k) - F(\arcsin (\sqrt{\gamma_1} \sin t), k)], \quad 0 \leq t \leq \frac{\pi}{2}; \quad (18)$$

$$l_1 = x(0) - l_0, \quad l_2 = \frac{2C}{\pi} \int_0^{\pi/2} \frac{t dt}{\sqrt{(1 - \alpha \cos^2 t)(1 - \gamma \cos^2 t)}}; \quad (19)$$

$$Q = \frac{C\rho K'}{\sqrt{\gamma_1}}; \quad (20)$$

$$T = \frac{2C}{\pi} \int_0^{\pi/2} \frac{\ln [(1 + \sqrt{\gamma_1 - (\alpha - \gamma) \sin^2 t}) / \sqrt{\gamma + (\alpha - \gamma) \sin^2 t}] dt}{\sqrt{\gamma_1 - (\alpha - \gamma) \sin^2 t}}; \quad (21)$$

$$H - \rho T = \frac{C\rho}{\sqrt{\gamma_1}} F\left(\arcsin \sqrt{\frac{\gamma}{\alpha}}, k\right), \quad (22)$$

where  $F$  is the elliptic integral of the first kind of the modulus  $k$  [4, 13].

In the case in question, the calculation control which is an analog of formulas (10)–(12) is the equality  $l_1 = L + l_2 - l_0$ ; the calculation is also controlled by the following expressions for the quantities  $T$  and  $H$ :

$$T = \frac{2A}{\pi} \int_d^e \frac{\ln (\sqrt{\zeta} + \sqrt{\zeta - 1}) d\zeta}{\sqrt{\zeta} (\zeta - 1) (\zeta - d) (e - \zeta)}, \quad H = \rho \left[ T + \frac{2A}{\sqrt{(e-1)d}} F\left(\arcsin \sqrt{\frac{d}{e}}, k\right) \right].$$

Taking into account that in this case the amplitude and modulus of elliptic integrals are related by the well-known relation ([14], p. 38)

$$\cot \arcsin \sqrt{\frac{e-1}{e}} \cot \arcsin \sqrt{\frac{d}{e}} = k',$$

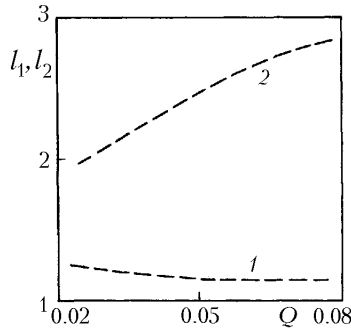


Fig. 5. Dependence of  $l_1$  and  $l_2$  on  $Q$  for  $T = 2.4$  m,  $\rho = 0.01$ , and  $H = 0.036$  m.  $l_1$  and  $l_2$ , m.

we may transform the expression in square brackets on the basis of (17) as follows:

$$F\left(\arcsin \sqrt{\frac{e-1}{e}}, k\right) + F\left(\arcsin \sqrt{\frac{d}{e}}, k\right) = K.$$

As a result of convolution, the right-hand sides of formulas (16) and (22) for  $H$  coincide, which is additional evidence in favor of the validity of formulas (16), (17), and (22).

**Analysis of the Numerical Calculations and Comparison of the Results for Both Schemes.** The representations (16)–(22) contain the unknown constants:  $C$ ,  $\gamma$ , and  $\alpha$  ( $0 \leq \gamma \leq \alpha < 1$ ). The  $Q/H$  ratio is used to determine the elliptic-integral modulus  $k = \sqrt{\alpha_1/\gamma_1}$ : from expressions (16) and (20) we obtain

$$\frac{K'}{K} = \frac{Q}{H}. \quad (23)$$

Knowing the relationship between the constants  $\alpha_1$  and  $\gamma_1$  (by means of the modulus  $k$ ) and using one equation for  $H$  or  $Q$ , we find the parameters  $\alpha_1$  and  $\gamma_1$  and hence  $\alpha$  and  $\gamma$ . In so doing, the constant  $C$  is eliminated, as before, from all Eqs. (16)–(22) by means of the expression for the stratum thickness  $T$ .

Relation (23) regulates prescription of the determining parameters  $Q$  and  $H$  and consequently the range of applicability of the flow diagram adopted. Therefore, unlike the scheme of lateral inflow, here it is more convenient to prescribe precisely the parameter  $Q$  which is determining in solving Eq. (23) instead of the stratum width  $L$  in numerical calculations and thereafter find the quantity  $L$ .

Figure 4 shows the flow pattern calculated for the same values of the parameters  $T$ ,  $H$ , and  $\rho$  as those in Fig. 1 and for  $Q = 0.055$ . The dimensions of the wedge  $l_1$  (curves 1) and  $l_2$  (curves 2) as functions of the determining physical parameters  $T$ ,  $\rho$ ,  $H$ , and  $Q$  are presented by the dashed curves in Figs. 3a–c and 5. An analysis of the dependences of the dimensions of intrusion on the physical characteristics is reduced to the following.

As in the previous problem, a growth in the thickness of the stratum leads to an increase in the dimensions of the wedge. It is remarkable that the dependence of the width  $l_1$  on  $T$  here is qualitatively similar to the dependence in the case of lateral inflow (Fig. 3a), and the dependences of  $l_1$  on  $\rho$  and  $H$  are linear (Fig. 3b and c). However, the character of the dependence of the quantity  $l_2$  with variation of  $\rho$  and  $H$  fundamentally changes compared to the first scheme: the growth in  $l_2$  is determined now by the decrease in the density of saline water and the increase in the acting head (Fig. 3b and c) and in the flow rate, which, in turn, is due to the decrease in the stratum width. It is noticeable that, as the parameters  $T$ ,  $\rho$ ,  $H$ , and  $Q$  change, the value of  $l_2$  varies within 41.6–85.5%, and it is changed to the greatest extent with variation of  $\rho$ , decreasing 1.85 times.

A significant influence on the quantity  $l_2$  is exerted, as before, by the stratum thickness  $T$ . It is seen that the increase in the head and the decrease in the flow rate lead to significant changes in the stratum thickness  $L$ : variations of the parameters  $H$  and  $Q$  yield an increase of 765 and 848% in  $L$  respectively.

The calculations show that for the values of the parameters given in Figs. 3 and 5 we have  $0.4 \leq l_1^{(2)}/l_2^{(1)} \leq 15$  and  $1.5 \leq l_2^{(2)}/l_2^{(1)} \leq 50$ , where the superscript indicates the computations by the first or second scheme. Those in-



equalities mean that in the problem on inflow from below, the quantity  $l_2$  is at least 1.5 times larger than the wedge height in the problem on lateral inflow.

From the plots of Figs. 3a–c and 5 it follows that we have  $l_1 < l_2$  for the calculated variants, i.e.,  $L < l_0$ . The latter shows that the abscissa of point B (left-hand boundary of the sea) in the flow plane is smaller than the abscissa of point F (separation of the boundary line from the water confining stratum). Moreover, it turns out that  $l_1 < l_0$ , too. As the parameters  $T$  and  $H$  increase and  $\rho$  and  $Q$  decrease, point F moves to increasingly larger distances to the right; it attains the largest distance with variation of the head: in this case the quantity  $l_0$  increases 3.4 times.

The ratio  $r = l_1/(l_0 + l_1)$  characterizing to a certain degree the curvature of the boundary line or its flattening-out decreases with decrease in the parameters  $T$ ,  $\rho$ , and  $Q$  and increase in  $H$ : this line is steeper for low values of the quantity  $r$ , but as  $r$  increases, the curve is gradually flattened out and becomes more extended to the right. Thus, it follows from the calculations that the parameter  $r$  decreases from 0.4198 to 0.1614 with increase in the head  $H$ , i.e., the boundary line becomes 2.6 times steeper.

When points D and E merge together in the  $z$  and  $\zeta$  planes, which corresponds to the values  $L = \infty$  and  $d = e$ , we have flow in a semiinfinite pressure water-bearing layer. The results for this case are obtained from formulas (16)–(22) for  $\alpha = \gamma$ ,  $k = 1$ , and  $k' = 0$ :

$$T = \frac{C}{\sqrt{\alpha_1}} F(\arcsin \sqrt{\alpha_1}, 1) = \frac{2A\alpha}{\sqrt{\alpha_1}} \ln \frac{1 + \sqrt{\alpha_1}}{\sqrt{\alpha}}, \quad Q = \frac{C\rho K'}{\sqrt{\alpha_1}} = \frac{A\rho\alpha\pi}{\sqrt{\alpha_1}}. \quad (24)$$

Here we have used a well-known result ([15], p. 37). The last formulas enable us to express the unknown constants in explicit form:

$$\alpha = \cosh^{-2} \frac{\pi\rho T}{2Q}, \quad A = \frac{Q}{2\pi} \sinh \frac{\pi\rho T}{Q}. \quad (25)$$

Expressions (25) coincide with (6.6) from [2] and are used for determination of the unknown parameters from the prescribed values of the physical characteristics  $T$  and  $Q$ .

**Conclusions.** We have found the exact analytical solutions of problems of intrusion of sea saline water into the littoral sweet-water horizons in the case of both the groundwater-flow entering the sea from the side (according to the scheme of Polubarinova-Kochina and Mikhailov) and tapering into the sea floor from below (according to the Bear–Dagan scheme traditional for problems of such kind). It has been established by means of numerical calculations that increase in the dimensions of the stratum and in the density of saline water and the thickness of its layer in the sea and decrease in the head lead to a growth in the dimensions of the saline-water wedge penetrated into the sweet-water stratum. In the second case, conversely, increase in the width of tapering into the sea floor is due to the decrease in the density of saline water and increase in the acting head.

It has been shown that for one set of particular values of the unknown parameters of conformal mappings, which are contained in the solution, we obtain from it the well-known results of P. Ya. Polubarinova-Kochina for the classical problem on filtration in a rectangular bridge.

The author is grateful to Academician of the Russian Academy of Sciences G. G. Chernyi and Professor S. A. Isaev for their attention expressed during this work and for useful remarks.

## NOTATION

$c$ ,  $d$ , and  $e$ , unknown affixes (i.e., images) of points C, D, and E on the auxiliary-variable plane in mapping by the function  $z(\zeta)$ ;  $F$ , elliptic integral of the first kind;  $H$ , acting head, m;  $k$ , modulus of elliptic integrals;  $k'$ , additional modulus;  $K$ , complete elliptic integral of the first kind of the modulus  $k$ ;  $K'$ , complete elliptic integral of the first kind of the additional modulus  $k'$ ;  $m$ , proportionality factor for the dimensions of the saline-water wedge;  $L$ , stratum width, m;  $l$ , dimension of the saline-water wedge, m;  $l_1$ , width of the saline-water wedge, m;  $l_2$ , height of the saline-water wedge, m;  $l_0 = L - l_1$ ;  $Q$ , total flow rate;  $Q_{BC}$ , rate of flow through portion BC;  $T$ , stratum thickness, m;  $t$ , water level in the sea, m;  $x$ , abscissa of a point of the region of flow, m;  $y$ , ordinate of a point of the region of

flow,  $m$ ;  $z$ , complex coordinate of a point of the region of flow;  $w$ , complex flow velocity;  $\zeta$ , auxiliary parametric variable;  $\kappa$ , filtration coefficient;  $\rho_1$ , density of sweet water,  $\text{g/cm}^3$ ;  $\rho_2$ , density of saline water,  $\text{g/cm}^3$ ;  $\rho = \frac{\rho_2}{\rho_1} - 1$ , dimensionless quantity;  $\varphi$ , velocity potential;  $\phi$ , stream function;  $\omega$ , complex flow potential.

## REFERENCES

1. G. K. Mikhailov, An exact solution of the problem on efflux of groundwater from a horizontal bed into a basin with a heavier fluid, *Dokl. Akad. Nauk SSSR*, **110**, No. 6, 945–948 (1956).
2. E. N. Bereslavskii, Study of flow filtration in some flows in the littoral water-bearing beds, *Prikl. Mat. Mekh.*, **67**, Issue 5, 836–848 (2003).
3. E. N. Bereslavskii, Calculation of filtration of groundwater in littoral pressure strata, *Izv. Ross. Akad. Nauk, Mekh. Zhidk. Gaza*, No. 3, 101–110 (2004).
4. P. Ya. Polubarinova-Kochina, *The Theory of Motion of Groundwater* [in Russian], Gostekhizdat, Moscow (1952); 2nd edn., Nauka, Moscow (1977).
5. V. V. Golubev, *Lectures on Analytical Theory of Linear Differential Equations* [in Russian], Gostekhizdat, Moscow, Leningrad (1950).
6. P. Ya. Polubarinova-Kochina, *Some Problems of Plane Motion of Groundwater* [in Russian], Izd. AN SSSR, Moscow, Leningrad (1942).
7. P. Ya. Polubarinova-Kochina, Calculation of filtration through a ground bridge, *Prikl. Mat. Mekh.*, **4**, No. 1, 53–64 (1940).
8. V. I. Aravin and S. N. Numerov, *Filtration Calculations of Hydraulic Engineering Structures* [in Russian], Gostekhizdat, Moscow, Leningrad (1955).
9. P. Ya. Polubarinova-Kochina, Concerning filtration in anisotropic ground, *Prikl. Mat. Mekh.*, **4**, No. 2, 101–104 (1940).
10. J. Bear, D. Zaslavsky, and S. Irmay, *Physical Principles of Water Percolation and Seepage* [Russian translation], Mir, Moscow (1971).
11. G. K. Mikhailov and V. N. Nikolaevskii, Motion of liquids and gases in porous media, in: *Mechanics in the USSR for 50 Years* [in Russian], Vol. 2, Nauka, Moscow (1970), pp. 585–648.
12. P. Ya. Kochina, E. N. Bereslavskii, and N. N. Kochina, *Analytical Theory of Linear Equations of the Fuks Class and Some Problems of Underground Hydromechanics* [in Russian], Preprint No. 567 of the Institute of Problems in Mechanics, Russian Academy of Sciences, Pt. 1, Moscow (1996).
13. I. S. Gradshteyn and I. M. Ryzhik, *Tables of Integrals, Sums, Series, and Products* [in Russian], Nauka, Moscow (1971).
14. A. M. Zhuravskii, *Handbook of Elliptical Functions* [in Russian], Izd. AN SSSR, Moscow, Leningrad (1941).
15. Yu. S. Sikorskii, *Elements of the Theory of Elliptical Functions with Applications* [in Russian], ONTI, Moscow, Leningrad (1936).